On vibration absorbers for vibration and noise attenuation for the fuselage and cabin of selected tonal engine disturbance, based on ground measurements

Michael Rose[a], Malte Misol[a]

[a] German Aerospace Center (DLR), Institute of Lightweight Systems, Lilienthalplatz 7, 38108 Braunschweig, Germany, e-mail: **michael.rose@dlr.de**,

Engine noise is of substantial impact on the passenger's comfort of modern airplanes. Besides the jet noise, certain selected tonal engine frequencies can be clearly observed as acoustic noise in the cabin. Based on ground measurements on a Dassault Falcon 2000LX MSN 006 airplane, three of these tonal frequencies have been identified and strategies have been developed to attenuate these frequencies with active and passive solutions subsequently. In this paper, the principal properties of vibration absorbers, mounted at one pylon, have been investigated, based on the spectral disturbances and frequency response functions, obtained from the ground test measurements. Using a vibration absorber at the pylon between the engine and the fuselage is suggested by the idea, to at least attenuate the structure borne noise of this path. The main focus of the presented study reveals the principle possibilities and restrictions of using vibration absorbers to vibration reduction on certain parts of the fuselage and on sound power reduction in certain cabin areas. Due to the fact, that only one position for an absorber was available from the underlying measurement data, numerical results are only available for one absorber at a fixed location. As part of the conclusion of the paper, using multiple absorbers would be mandatory to gain sufficient global attenuation, but the principles can be demonstrated fairly well with the chosen set up.

1 Introduction

The ISTAR (In-Flight Systems & Technology Airborne Research, figure 1) is a business jet from Dassault Aviation that was reconditioned as a research platform and is part of the DLR's fleet since 2020. It is a long-range variant of the Falcon 2000EX with the addition of blended winglets.

Figure 1: ISTAR Falcon 2000LX MSN 006

Some geometrical and physical parameters are given by

Length	20.2 m
Height	7.1 m
Wing span	21.4 m
Maximum Speed	961 km/h
Range	7400 km
Total Weight	19140 kg
Max. Flight Altitude	14300 m
2 Engines	Pratt & Whitney PW 308C

To study different noise control systems applicable to this airplane, a vibroacoustic test (VAT) was performed in March 2022 at DLR site in Braunschweig. Two different noise control approaches are considered: Active Noise Vibration Control (ANVC) with intertial exciters applied to interior parts of the cabin (see [1, 2]) and Tuned Vibration Absorbers (TVA) acting on the pylons. This paper is focussed on the second approach to discuss its principal properties and limitations. During the VAT, Frequency Response Functions (FRF) of electrodynamic shakers to accelerometers and microphones are determined by means of multi-reference tests. The TVA's are principally suitable to attenuate narrow band noise like certain tonal frequencies within the spectrum. Three main tonal frequencies of interest (137 Hz, 273 Hz and 403 Hz) have been investigated in this study. Two fixed positions at the bottom of one pylon have been included in the measurements (exciters with integrated force sensors, see figure 2). The closer one nearest to the airplane front was used in the study. One shortcoming in the first test campaign, from which the main results are based upon, is the fact, that no true collocated accelerometer was available directly at the TVA position. The nearest available accelerometer was at a distance of 40 cm (yellow patch in the figure), which invalidates the needed phase information of the excitation. A second test campaigne was equipped with true collocated actuators and sensors.

2 Tunable Vibration Absorber

A tunable vibration absorber is a device consisting of a mass, which is mounted to the structure with some kind

Figure 2: Two fixed TVA position at the bottom of the pylon, airplane front is left in picture

of damped spring. Its oscillation frequency is tuned to be in the proximity of a structural eigenfrequency, and with properly chosen mass stiffness and damping, the resonance peak of the structure can be significantly reduced. The amount of possible reduction is dependent on the ratio of the absorber mass and the modal mass of the considered structural eigenfrequency. In figure 3 a schematic

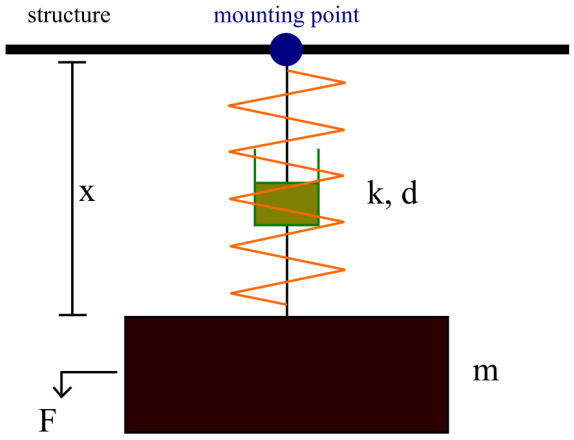

Figure 3: Schematic of a tunable vibration absorber

of a single degree of freedom vibration absorber is displayed, which is introducing transversal forces into the structure at the mounting point. Other physical layouts exist of course; forces in surface direction can be generated as well as moments with a rotational spring stiffness and rotational inertia. Even TVA based on structurally integrated piezoelectric devices and suitable electrical networks have been realized (see [3]). But they all act locally and collocal on the structure. In this project, the exciter was setup to generate transversal forces orthogonal to the pylon of the airplane in z-direction (up). Therefore, the investigation is focused on the displayed type of absorber.

2.1 Basic absorber characteristics

To investigate absorbers, which are capable of reducing a structural eigenmode, the multi degree of freedom (DOF) system is first reduced to a single DOF, which represents the eigenmode under consideration. There are multiple methods to get such a simplified system FRF from the full bandwidth FRF. The simplest one is the half bandwidth criterium, but for more accuracy, the Nyquist circle criterium or even more sophisticated methods can be used (see [4] for details). The single DOF system is characterized by its modal mass m_0, damping d_0 and stiffness k_0. A harmonic force F transversal to the structure will induce a corresponding harmonic transversal displacement x_0. The FRF of the single DOF system is then given by the fraction

$$\frac{x_0}{F} = \frac{1}{m_0 s^2 + d_0 s + k_0} \tag{1}$$

with $s = i\omega$ and the angular frequency ω. If we add an absorber with mass m_1, damping d_1 and stiffness k_1 to this system and denote the absolute absorber mass position by x_1, the augmented system in the frequency domain is given by

$$(m_0 s^2 + d_0 s + k_0)x_0 + (d_1 s + k_1)(x_0 - x_1) = F, \tag{2}$$
$$m_1 s^2 x_1 + (d_1 s + k_1)(x_1 - x_0) = 0. \tag{3}$$

Or by substituting the second equation into the first one

$$(m_0 s^2 + d_0 s + k_0)x_0 + m_1 s^2 x_1 = F, \tag{4}$$
$$(m_1 s^2 + d_1 s + k_1)x_1 = (d_1 s + k_1)x_0. \tag{5}$$

Usually it is advantageous to transform these equations to a dimensionless form. With

$$\mu = \frac{m_1}{m_0}, \omega_0 = \sqrt{\frac{k_0}{m_0}}, \omega_1 = \sqrt{\frac{k_1}{m_1}}, \delta = \frac{\omega_1}{\omega_0},$$
$$\xi_0 = \frac{d_0}{2m_0\omega_0}, \xi_1 = \frac{d_1}{2m_1\omega_1}, f = \frac{F}{k_0}, s = \omega_0\gamma, \tag{6}$$

the dimensionless absorber equations are given by

$$\frac{x_0}{f} = \frac{S_1}{S_0 S_1 + \mu S_2 \gamma^2}, \quad \frac{x_1}{x_0} = \frac{S_2}{S_1}, \tag{7}$$

$$\begin{bmatrix} S_0 \\ S_1 \\ S_2 \end{bmatrix} = \begin{bmatrix} \gamma^2 + 2\xi_0\gamma + 1 \\ \gamma^2 + 2\delta\xi_1\gamma + \delta^2 \\ 2\delta\xi_1\gamma + \delta^2 \end{bmatrix}. \tag{8}$$

The quantities are described in table 1. Usually there are application dependent restrictions on the upper limit for the mass ratio μ. A higher value will induce more damping to the structure, but it also increases the mass

Table 1: Absorber quantities

μ	mass ratio absorber/system
δ	frequency ratio absorber/system
ξ_0	system damping ratio
ξ_1	absorber damping ratio
ω_0	system angular frequency
ω_1	absorber angular frequency
f	relative force (static deflection)
$\gamma = i(\omega/\omega_0)$	complex frequency variable

added by the absorber. A suitable value is generally prescribed. The optimal values for the spring stiffness and damping of the absorber, indirectly given by the dimensionless quantities δ and ξ_1 can be obtained by an optimization procedure, which minimizes the maximum of the real rational function

$$\left|\frac{x_0}{f}\right|^2 \quad \text{in} \quad \frac{\omega}{\omega_0}. \tag{9}$$

For small damping, there are some approximate formulas for the absorber parameter. Given some mass ratio, the dimensionless frequency and damping of the absorber can approximately be calculated from

$$\delta = \frac{1}{1+\mu}, \quad \xi_1 = \sqrt{\frac{3\mu}{8(1+\mu)^3}} \tag{10}$$

(see [5]). These estimates can also be used to start a nonlinear optimization process to further fine tune them.

2.2 Absorber design on the pylon

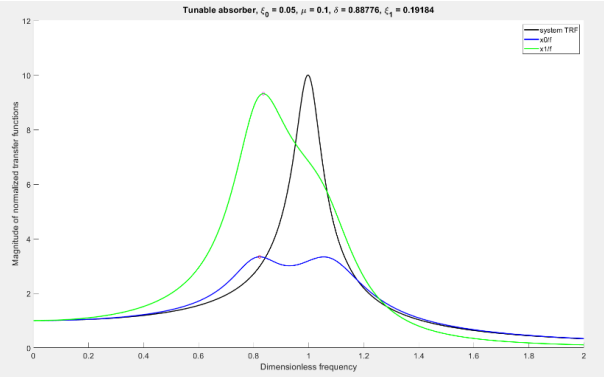

Figure 4: Example of a TVA (dimensionless plot)

One example of such an optimization is displayed in figure 4. It can be observed, that a significant vibration reduction in the FRF can be achieved, if the structural damping of the corresponding eigenmode is low. If the system behavior is not really constant (e.g. variations due to temperature changes), it is advisable to implement so called adaptive tunable absorbers. These adaptive designs need an outer control loop, which changes the parameters (usually only the stiffness) of the absorber to keep it in optimal operation condition. In figure 5 the shaker position at the pylon is displayed in relation to the sensor mesh on the fuselage. A collocal acceleration sensor was available for the measurement of the collocal FRF. However, for the engine noise, this sensor was not available. The closest point near the shaker point for excitation FRF is also displayed in the figure.

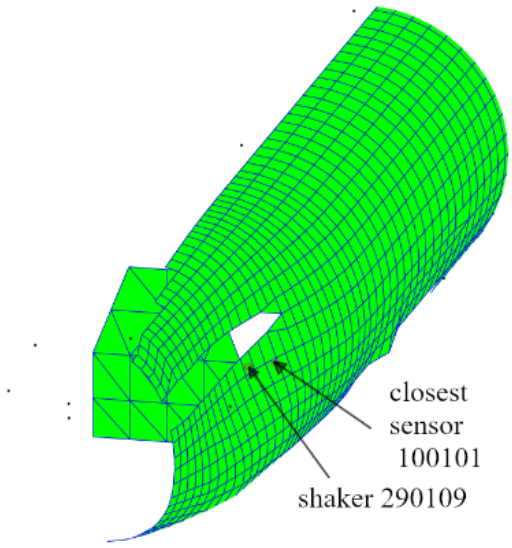

Figure 5: Location of shaker point and closest sensor point

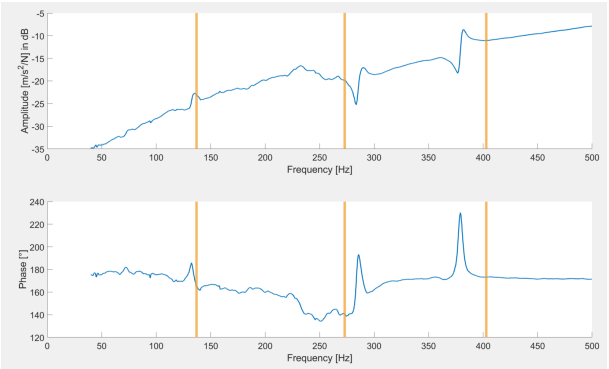

Figure 6: Bode plot of collocal FRF (point 290109)

In figure 6 the bode plot of the collocal FRF from force to transversal displacement at the shaker point on the pylon of the airplane is displayed. The excitation direction is the $+z$-direction (up). The orange lines indicate the tonal peak frequencies of the engine. In figure 7 the spectrum of the engine noise at point 100101 near the ab-

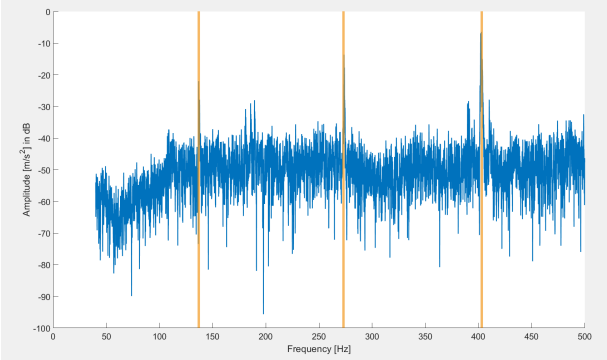

Figure 7: Engine noise at closest sensor point 100101

sorber position on the pylon is displayed (about 39,1cm distance). In combination it can be seen, that there are no significant resonance frequencies in the pylon FRF at the tonal peak frequencies of the engine. In figure 8

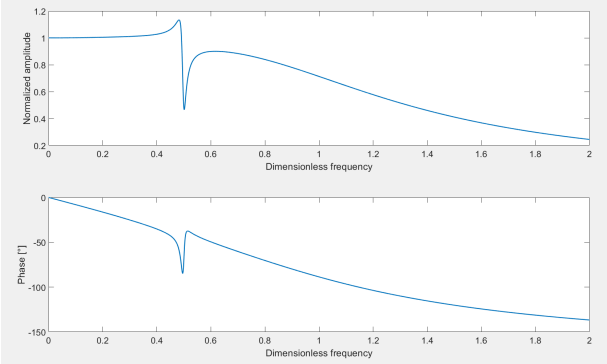

Figure 8: Effect of an absorber outside of resonance ($\mu = 0.1$, $\xi_0 = 0.7$, $\xi_1 = 0.07$, $\delta = 0,5$)

the effect of an absorber with absorber frequency distant from any structural resonance frequency is shown. The FRF clearly shows, that the absorber has a local effect, but there is a small region of amplification below the absorber frequency and a small region of attenuation above the absorber frequency. An absorber design is still possible, but there will be no global effect. In general, it can be expected, that for some sensor points a damping effect can be achieved if the absorber is dimensioned with these sensors in mind. An adaptive absorber is also beneficial in this scenario to keep the small frequency range of the absorber with attenuation in the possibly slightly changing target range.

For general operational vibrations at non-resonance frequencies, we generalize the equations of section 2.1, replacing the single DOF assumption by general FRFs. In addition, the accelerations $a_0 = s^2 x_0$ and $a_1 = s^2 x_1$ are used directly. In combination with the accelerations $a_0^d = s^2 x_0^d$ due to engine forces, the system equations are given by

$$a_0 = g_0 F + a_0^d, \tag{11}$$
$$F = -h a_0, \tag{12}$$
$$h = m_1 \frac{a_1}{a_0}, \tag{13}$$
$$0 = m_1 a_1 + (d_1 s + k_1)(x_1 - x_0) \tag{14}$$

with the general collocal transfer function $g_0(s)$ at the absorber location with respect to accelerations and the absorber transfer function $h(s)$. For the special case of a SDOF mass damper system, this specializes to

$$g_0(s) = \frac{s^2}{m_0 s^2 + d_0 s + k_0}, \tag{15}$$
$$h(s) = m_1 \frac{2\delta\xi_1\gamma + \delta^2}{\gamma^2 + 2\delta\xi_1\gamma + \delta^2}, \tag{16}$$
$$a_0 = \frac{a_0^d}{1 + g_0 h}, \tag{17}$$
$$F = -h a_0. \tag{18}$$

It is straight forward to verify, that the equations for SDOF of section 2.1are a special case of this relation for positions instead of accelerations (just insert the SDOF $g_0(s)$ and substitute $a_0^d = g_0 \hat{F}$ with the external excitation force $\hat{F}$).

In a qualitative assessment, the influence of the absorber increases with increasing values of h. This can be achieved either by increasing the absorber mass m_1 and by tuning the absorber frequency to be near the operational frequency ω_0, e.g. $\delta \approx 1$. At the operational frequency ($\gamma = i$), the mass and stiffness terms approximately cancel each other ($\gamma^2 + \delta^2 \approx 0$). This results in

$$h \approx -\frac{m_1}{2\xi_1} i, \quad a_0 \approx \frac{a_0^d}{1 - g_0 \frac{m_1}{2\xi_1} i}. \tag{19}$$

The special case of SDOF with small damping ξ_0 leads to the following qualitative relations

$$g_0 = \frac{1}{m_0} \frac{\gamma^2}{\gamma^2 + 2\xi_0\gamma + 1} \approx \frac{i}{2\xi_0 m_0}, \tag{20}$$
$$a_0 \approx \frac{a_0^d}{1 + \frac{m_1}{4 m_0 \xi_0 \xi_1}} = \frac{a_0^d}{1 + \frac{\mu}{4\xi_0\xi_1}}. \tag{21}$$

As a general result, the vibrations cannot be cancelled completely at an optimally tuned operational frequency. The mass ratio μ with respect to the absorber mass m_1 and the modal structural mass m_0 is directly related to the achievable vibration reduction for lightly damped structures and absorbers. In this case, a reduced damping also increases the absorber influence.

The above discussion is focused on the collocal absorber behavior. The influence on distant points is strongly dictated by the relative phase differences between the absorber forces and the disturbance on each structural point.

In general, this implies that an absorber might only positively affect small distant regions and can simultaneously negatively affect other regions of the structure if these phases are not correlated. If the main disturbance path is structure-borne noise and the coupling of the absorber into the structure is able to influence this path (non-orthogonal coupling), there is a bigger chance, that a global attenuation affect can be gained by an absorber in the direct frequency neighborhood of the tonal disturbance ω_0.

So far only one single absorber has been discussed. It is principally straightforward to use multiple TVA and superposition to overlay the effects. Complications only arise by the induced multi parameter optimization of the TVA parameters. Due to lack of experimental data and for simplicity, the usage of multiple TVA is not further discussed in this paper.

3 Results

To design a TVA for a specified tonal frequency, the collocal FRF at the absorber location and the FRF from the absorber location to the distant attenuation observer point must be available. In addition, the engine spectrum at the absorber location as well as at the observer point must be given. Unfortunately, in the first measurement campaign, the excitation spectrum was only available near the absorber location (distance 39.1 cm). This leads to some weaker statements due to lack of consistent phase information.

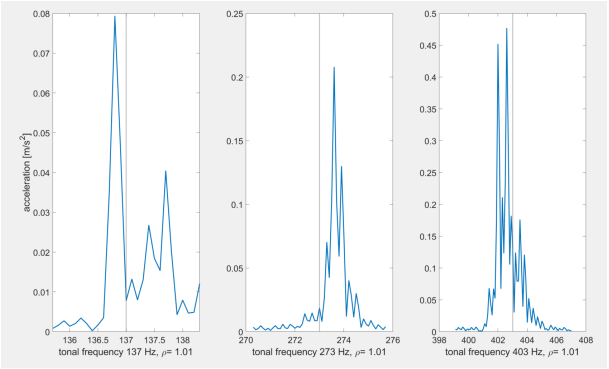

Figure 9: Engine excitation at closest sensor point to TVA

In figure 9 the local frequency range around the three selected tonal engine disturbance frequencies are displayed. In figure 10 the L2-mean value of accelerations on the fuselage due to engine noise is shown. The goal is to design an absorber for each of these frequency ranges with different masses to attenuate the engine accelerations. The corresponding collocal transfer function $g_0(s)$ at the absorber location is displayed in figure 11. In figure 12 the optimal dimensionless absorber parameters δ

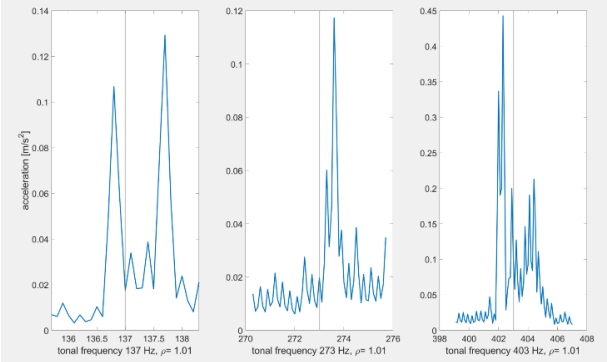

Figure 10: L2-mean engine excitation at fuselage sensor points

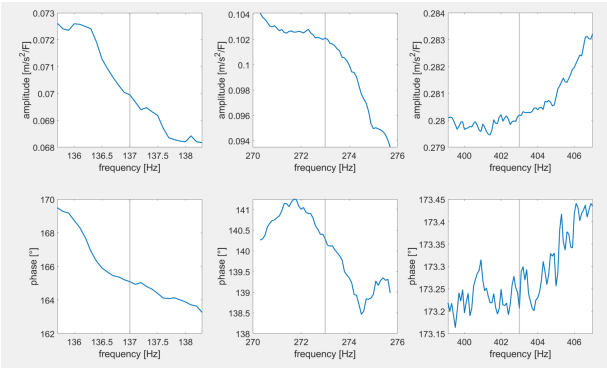

Figure 11: Transfer function $g_0(s)$ with $a_0 = g_0 \cdot F$

and ξ_1 for different absorber masses m_1 are displayed in the neighborhood of each of the three main tonal engine disturbances. Naturally, $\delta \approx 1$, because the eigenfrequency of the absorber is near the frequency of interest where attenuation of the accelerations is possible. There are some discontinuities in the curves, because the optimization is done on a discrete grid and the optimum functional is flat in some regions. In addition, the lower bound for the absorber damping was bound by the minimum relative damping of 0.001. For some transfer functions $g_0(s)$, the best possible value is in fact zero damping, e.g. $\xi_1 = 0$, but the change in the optimal attenuation is usually small for low absorber damping ratios. In figure 13 the attenuation of the collocal engine disturbance is displayed for the mass variation and the optimal absorber parameters. We have about 50% reduction with masses around 500 g, 660 g and 110 g for the three main tonal engine frequencies. For 90% reduction, masses of 2.7 kg, 3.3 kg and 0.7 kg will be sufficient.

In figure 14 the acceleration and force ratios a_1/a_0^d and F/a_0^d are displayed. These can be used to conservatively estimate the maximum absorber forces and absorber mass acceleration for representative collocal disturbance accelerations. A look into figure 9

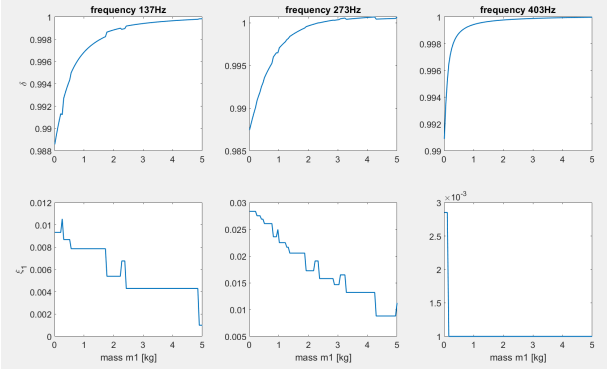

Figure 12: Absorber parameters δ and ξ_1 for different absorber masses m_1

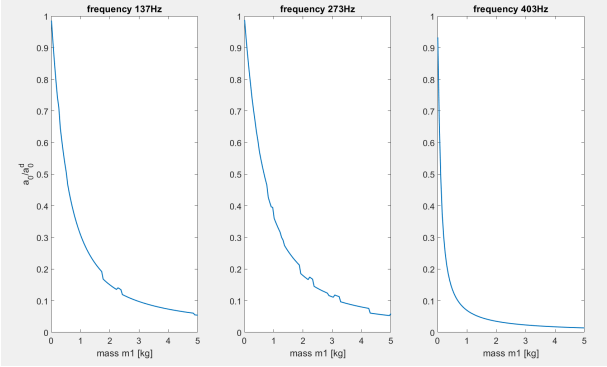

Figure 13: Collocal disturbance absorber attenuation a_0^d

shows characteristic accelerations of $0.08\,\mathrm{m/s^2}$, $0.2\,\mathrm{m/s^2}$ and $0.5\,\mathrm{m/s^2}$ at the main tonal frequencies. This leads to forces in the order of 1-2 N, which are brought into the structure by the absorber itself. The absorber mass acceleration is larger for low absorber damping ratios and lower absorber masses. In combination with the characteristic accelerations, accelerations in the order of $1\,\mathrm{m/s^2}$ are rough estimates for these absorber mass acceleration amplitudes. The frequency range 100-400 Hz leads to positional amplitudes in an acceptable range for the chosen masses.

For this discussion, the disturbance acceleration at the closest point 100101 was used as collocal disturbances at the shaker location 290109. The points are about 39,1cm apart, which leads to additional errors. Unfortunately, there was no collocal measurement for the engine noise in the first measurement campaign. The errors introduced by this choice are hard to predict, because the phase of a_0^d influences the phase of the forces and therefore the attenuation at other points of the structure. In addition, the phases of a_0^d to other disturbance accelerations are not known, because the accelerations at the closest point 100101 were obtained by a different measurement set than the accelerations at the choosen fuselage measure-

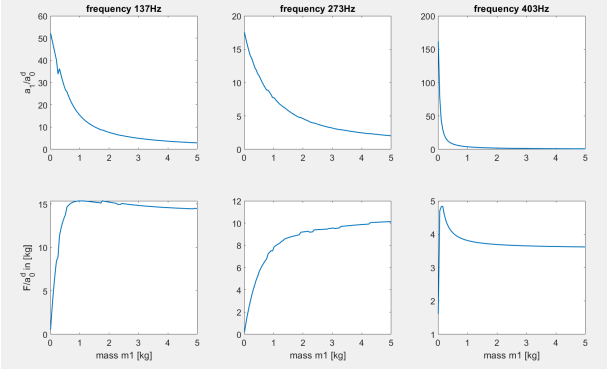

Figure 14: Absorber acceleration and force ratios wrt. the collocal disturbance attenuation a_0^d

ment points. Therefore, a prediction of non-collocal absorber attenuation is not reliably possible on the basis of the supplied measurement data.

But some inside on the feasibility of global attenuation with only one absorber at the pylon can still be gained. In figure 15 the acceleration of the first tonal frequency

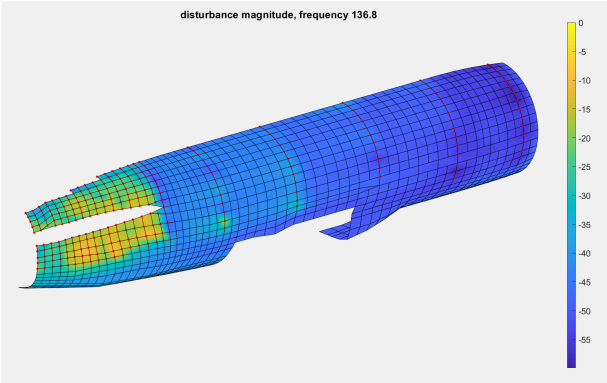

Figure 15: Engine disturbance acceleration in decibel for first tonal frequency

on a large part of the fuselage is displayed in decibel. In figure 16 the FRF's from forces at the absorber point to accelerations at the fuselage are displayed, also in decibel and for the first tonal frequency. For the second and third tonal frequency, similar pictures can be obtained. Vibrations clearly dominate at the rear part of the fuselage and the influence of absorber forces to the fuselage is also only significant in the neighborhood of the pylon. As a result, only the rear airplane section has a chance of noticeable disturbance attenuation due to an absorber located at the pylon.

In figures 17, 18 and 19 the distribution of the phase angles of the disturbance accelerations are displayed in degrees. To avoid angle wrapping, only the absolute value is shown. The areas of similar phase angles get smaller

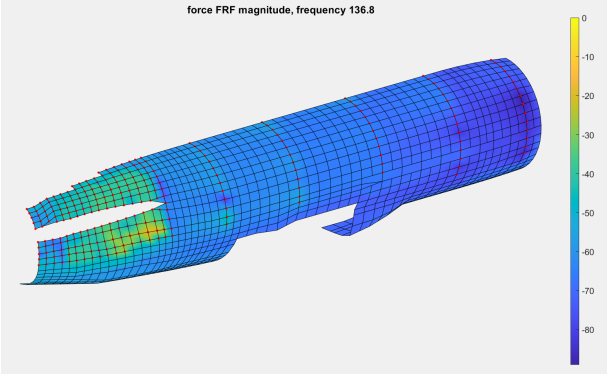

Figure 16: Force FRF (m/s^2/F) in decibel

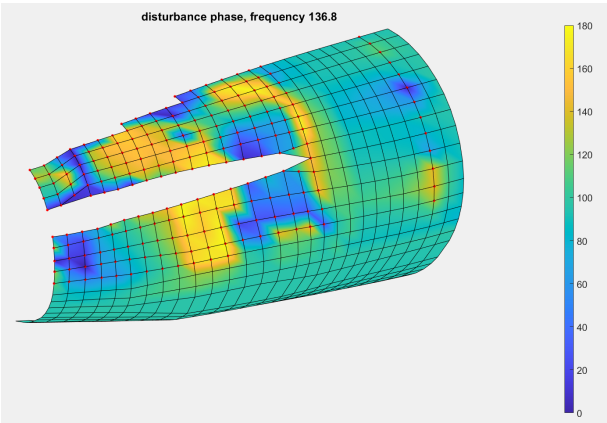

Figure 17: Phase of engine excitation for first tonal frequency

with increasing frequency. The pictures are heavily interpolated, because only a limited set of sensor points is available on the fuselage surface. But it is clearly observable, that all phase angles are present in the displayed surface section.

In figures 20, 21 and 22 the corresponding phase plots are displayed with respect to the force FRF from the absorber forces to the fuselage accelerations. There is also some phase variation in the displayed fuselage surface area, but there is no good coincidence to the phases displayed in figures 17, 18 and 19. To have the chance of global attenuation with one absorber, the surface section under consideration must have similar phase distribution, because only one absorber force will be available. This indicates, that global attenuation on the rear part of the fuselage will not be possible with only one TVA at the pylon.

Finally, the distribution of phase deviations between absorber induced accelerations and engine disturbance accelerations is displayed in figures 23, 24 and 25. The distribution indicates, that there is a certain possibility, that a single absorber can attenuate the blue surface area for the first tonal frequency 136.8 Hz. Due to the lack of phase

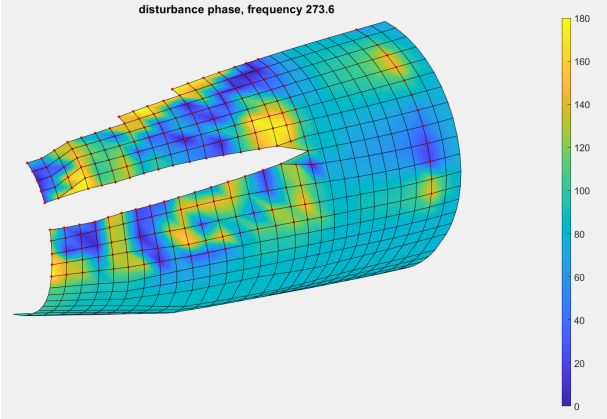

Figure 18: Phase of engine excitation for second tonal frequency

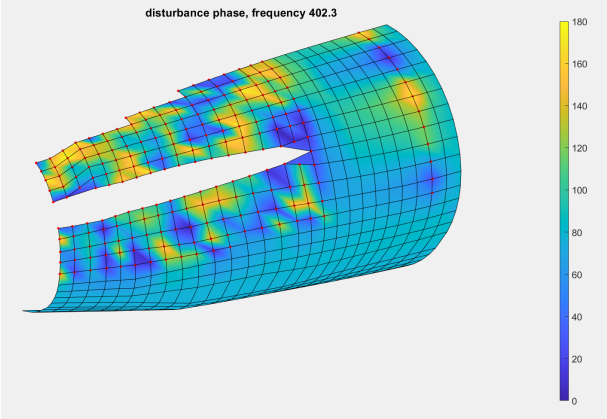

Figure 19: Phase of engine excitation for third tonal frequency

information for $a_0^d(s)$, it cannot be granted, that such an absorber is feasible. The other two pictures indicate, that global attenuation at frequencies 273,6 Hz and 402,3 Hz is not achievable with only one absorber.

4 Conclusion

To be able to design an absorber for a structure like the airplane in this study, the following data must be measured in the neighborhood of the tonal frequency f_0, which should be attacked:

- The collocal FRF $g_0(s)$ with $a_0(s) = g_0(s)F(s)$ at the mounting point of the absorber. The crucial point is the collocal setup of F and a_0. Not only transversal forces and accelerations can be used, also rotational or other collocal DOF's are feasible.
- The collocal disturbances $a_0^d(s)$ at the absorber lo-

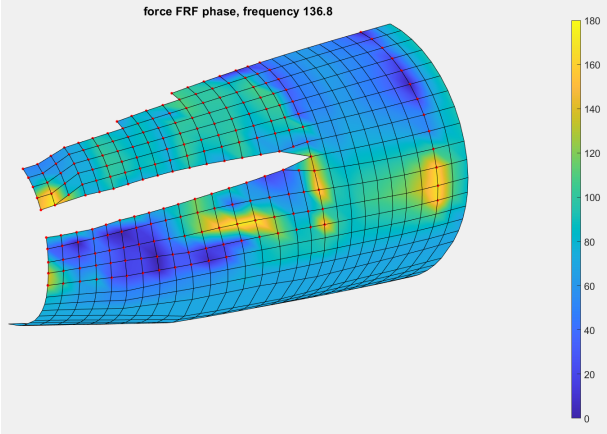

Figure 20: Phase of absorber FRF to fuselage for first tonal frequency

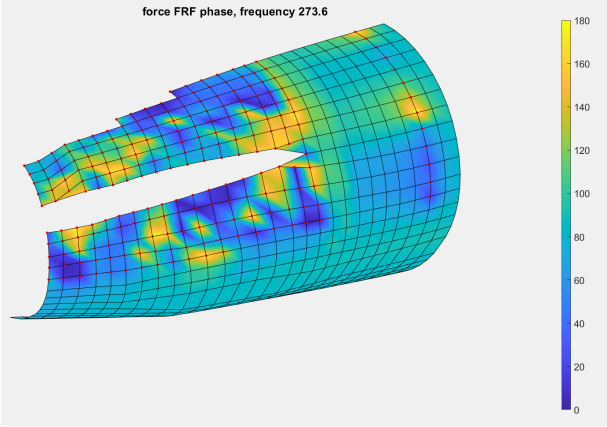

Figure 21: Phase of absorber FRF to fuselage for second tonal frequency

cation, introduced by noise sources at some other structural location (e.g. engine).

- Transfer functions (FRF) with forces at the absorber location to accelerations at each structural sensor point of interest.
- Disturbance accelerations at each of the chosen sensor points, which must by correct in phase with respect to each other and to the collocal disturbances $a_0^d(s)$.

A substantial attenuation of the disturbance accelerations at the absorber position is usually feasible. A reasonable absorber mass m_1 must be selected. The dimensionless absorber parameters $\delta \approx 1$ and $\xi_1 \ll 1$ can be calculated. This leads to physical stiffness and damping parameters for the absorber according to equation (6). In addition, the collocal attenuation ratio can be calculated. With the transfer functions $g_z(s)$ with $a_z(s) = g_z(s)F(s)$ at

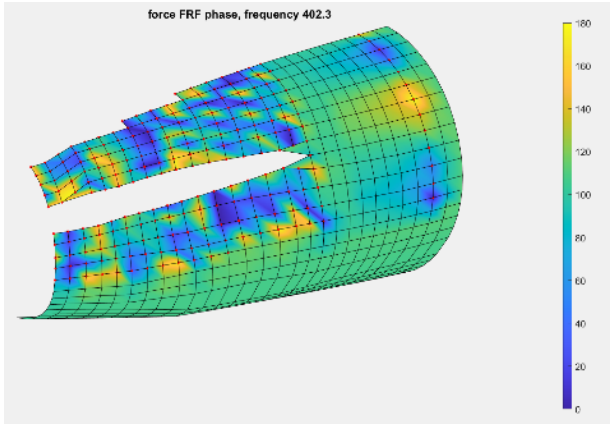

Figure 22: Phase of absorber FRF to fuselage for third tonal frequency

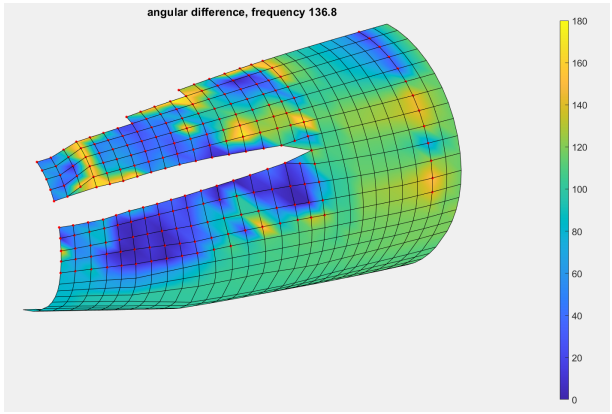

Figure 23: Phase difference of engine excitation and of absorber FRF for first tonal frequency

the chosen structural points and the disturbance accelerations $a_z^d(s)$, the change due to the absorber is given by $a_z(s) = g_z(s)F(s) + a_z^d(s)$, using the forces $F(s)$ introduced by the absorber with respect to the collocal disturbance accelerations $a_0^d(s)$. Whether a reduced acceleration (attenuation) can be achieved depends on the signal phases. If the disturbance is mainly induced by structure-borne noise and the wave path is influenced by the absorber position, a global attenuation can be possible. Otherwise, there will be regions of attenuation and regions with even larger acceleration amplitudes in the neighborhood of the tonal frequency under consideration.

This investigation was later refined by a second test campaign with truly collocal excitation spectrum at the absorber location. Instead of accelerometers on the fuselage, the observer sensors consist of 65 microphones in the cabin. An absorber design as above with the new measurements with location on the bottom of the right pylon with optimal parameters for the three tonal frequencies shows substantial effect on the collocal structural accel-

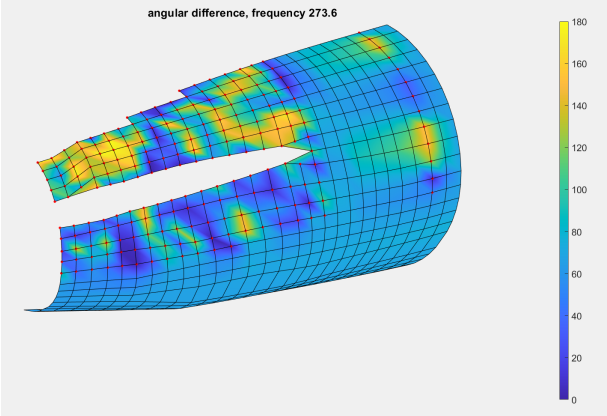

Figure 24: Phase difference of engine excitation and of absorber FRF for second tonal frequency

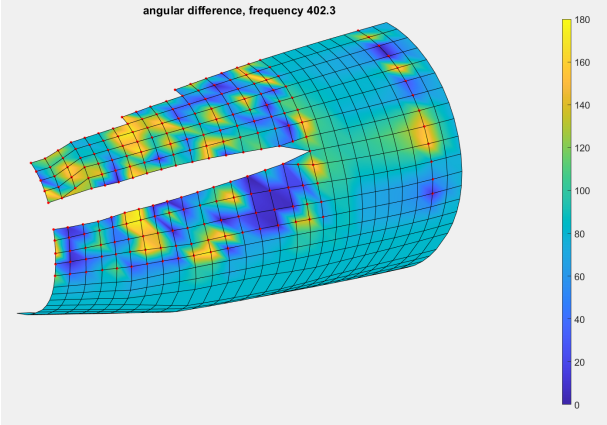

Figure 25: Phase difference of engine excitation and of absorber FRF for third tonal frequency

erations with attenuations within 10-20 dB in the direct neighborhood of the three tonal frequencies. This might also indicate local structural behavior with weak stiffness. A low stiffness usually disables good impact on distant structural parts. With one absorber — similar to the situation for the first test campaign wrt. the fuselage — no global sound attenuation is achievable at the microphones in the cabin.

5 Acknowledgement

The support of project partner Dassault Aviation is gratefully acknowledged.

This project has received funding from the Clean Sky 2 Joint Undertaking under the European Union's Horizon 2020 research and innovation programme under grant agreement N° CS2-LPA-GAM-2020-2023-01.

References

[1] M. Misol, S. Algermissen, H.P. Monner, U. Dinc,er, 'Design of an Active Noise Control System for a Business Jet with Turbofan Engines', *29th International Congress on Sound and Vibration (ICSV)*, pp. 1–8, ISBN 978-801103423-8, https://elib.dlr.de/195890/, Prague, Czech Republic (2023).

[2] M. Misol, U. Dinc,er, M. Prade, 'Smarte Verkleidungsteile für die Flugzeugkabine der Zukunft', Blog, https://leichtbau.dlr.de/smarte-verkleidungsteile-fuer-die-flugzeugkabine-der-zukunft (2024).

[3] N.W. Hagood, A. von Flotow, 'Damping of Structural Vibrations with Piezoelectric Materials and Passive Electical Networks', *Journal of Sound and Vibration*, Vol. 146, No. 2. pp. 243–268 (1991).

[4] D.J. Ewins, *'Modal Testing, Theory and Practice.'*, Research Studies Press, Ltd. Taunton, UK (1984).

[5] Maurer, 'Schwingungstilger und Viskodämpfer', *Maurer und Söhne*, Vol. 2, Stammhaus München (2011).